

# A FAST CONTEXTUAL CLASSIFIER FOR INFORMATION EXTRACTION FROM REMOTELY SENSED IMAGERY

P. Gong

Department of Surveying Engineering  
The University of Calgary  
Calgary, Alberta, Canada T2N 1N4  
Tel. (403) 220-5826 Fax. (403) 284-1980  
E-mail: gong@ensu.ucalgary.ca

## ABSTRACT:

A new contextual classifier has been developed and evaluated for information extraction from remotely sensed imagery. The algorithm is computationally very efficient, and experiment indicated that it can achieve more accurate results than the conventional maximum likelihood classifier and some commonly-used texture/contextual algorithms. The new contextual classifier includes two basic procedures: grey-level vector reduction and frequency-based classification. In grey-level vector reduction, the number of grey-level vectors in multispectral space is reduced using a new data-reduction algorithm through rotating multispectral space into eigen space. As a result, the multispectral data are reduced to images of one feature dimension with the loss of relatively little information. Each grey-level vector-reduced image is then used in the frequency-based procedure to derive useful information. The frequency-based classification procedure includes a grey-level vector occurrence-frequency extractor, a minimum-distance classifier and an accuracy evaluator. Landsat Thematic Mapper data have been used to illustrate the potential of the new algorithm. We have emphasized on land-use classification since land use is a cultural concept that is difficult to be mapped directly using remote sensing data. The potential of using the grey-level vector reduction algorithm for fast clustering has been discussed as well.

## 1. INTRODUCTION

Gong and Howarth (1992) has developed a frequency-based contextual classifier based on grey-level vector reduction in eigenspace. In comparison to other contextual classifiers, this algorithm is computationally efficient. They applied this method with the use of SPOT High Resolution Visible (HRV) data in the classification of land uses in a rural-urban fringe environment. They demonstrated that the frequency-based classifier was superior to not only the traditional maximum-likelihood classifier (MLC) but also a few other commonly-used contextual classification algorithms (Gong, *et al.*, 1992).

In this paper, the Cong-Howarth frequency-based contextual classifier has been applied to conduct land-use classifications of a urban environment similar to the one studied in Gong and Howarth (1992) using Landsat Thematic Mapper (TM) data. We will introduce the Gong-Howarth contextual classifier first and then report the classification results.

## 2. GONG-HOWARTH FREQUENCY-BASED CONTEXTUAL CLASSIFIER

### 2.1. OCCURRENCE FREQUENCIES AS A SURROGATE FOR SPATIAL FEATURES

Occurrence frequency,  $f_l(i,j,v)$ , is defined as the number of times that a pixel value  $v$  occurs in a pixel window centered at  $(i,j)$ . For computational simplicity, the pixel window has a square shape with a lateral length of  $l$  ( $l > 1$ ). For a single-band image,  $v$  represents a grey level. For multispectral images,  $v$  represents a grey-level vector. Within each pixel window, one can obtain an occurrence-frequency table containing all possible  $vs$ .

When a pixel window of a given size is moved all over an image(s), one can generate a frequency table for each pixel in the image(s), except for those pixels close to the image boundary. Those pixels within a distance to the image boundaries of half the lateral length,  $l$ , of the pixel window are called boundary pixels. Since full frequency tables cannot be obtained at boundary pixels, these pixel positions should be avoided in further analysis. To assure a small proportion of boundary pixels, the pixel window sizes used must be considerably smaller than the image size.

The number of occurrence frequencies in a frequency table increases linearly as the number of grey levels in an image increases, and exponentially as the number (or dimensionality) of spectral bands increases. For a single-band image quantized into  $n$  grey levels, one can produce grey-level occurrence frequency tables with a maximum number of  $n$  frequencies in each table. The maximum number of frequencies in a frequency table will increase to  $n^m$  when  $m$  spectral bands having the same number of grey levels are used. It requires a large amount of random access memory (RAM) in a computer to handle the  $n^m$  frequencies. For this reason, efficient grey-level vector-reduction algorithms are needed. One such algorithm will be introduced later in this paper. Frequency tables can be generated from grey-level vector-reduced images.

There are several advantages to using frequency tables when compared with the use of spatial statistical measures, as in spatial feature methods. First, a frequency table contains more spatial information than many statistical measures. For instance, the most commonly used statistical measures such as the mean, standard deviation, skewness, kurtosis, range, and entropy can all be derived from a grey-level frequency table. However, additional computation is required to obtain statistical parameters after the frequency tables are produced. Therefore, it becomes unnecessary to use statistical measures because frequency tables can be quickly computed, directly compared and analyzed. The second advantage is that the feature-selection procedure, which is used to evaluate statistical parameters, is no longer needed because frequency tables contain more spatial information required for the classification than the above statistical parameters. Third, disk storage is not required by frequency tables due to the simplicity of their real-time creation.

### 2.2. THE CLASSIFIER

The classifier used in this study is the minimum-distance classifier with the city-block metric (Gonzalez and Wintz, 1987). A city-block distance between two vectors is calculated by first obtaining a difference between every two corresponding vector elements, and then summing all the absolutes of these differences. There are two reasons for selecting the city-block distance. The first is that this distance is the simplest one in

terms of computation, and therefore it could be used to handle occurrence frequencies extracted from an image with more grey-level vectors. Second, since we are comparing frequencies to make the classification decision, the use of Euclidian distance or other metrics is meaningless. In fact, some preliminary tests have been made in this study to compare the performances of the city-block metric and the Euclidian metric. Overall accuracies were on average 5% higher in favor of the city-block metric.

For given mean histograms of all  $c$  land-use classes,  $h_u = (f_u(1), f_u(2), \dots, f_u(N_v))$ ,  $u = 1, 2, \dots, c$ , the city-block distance between a new histogram  $h_l(i, j)$  and  $h_u$  is calculated from the following:

$$d_u = \sum_{v=0}^{N_v} |f_u(v) - f(i, j, v)|$$

The classifier compares all the  $c$  distances and assigns pixel  $(i, j)$  to the class which has a minimum distance to  $h_l(i, j)$ .

### 2.3. PERFORMANCE ASSESSMENT

The most commonly used accuracy-assessment method is test-sample checking. It requires three steps: determination of sample size and sampling strategy, sample identification (ground confirmation) to generate reference data, and comparison of the reference data with classification results to derive classification accuracies. The first two steps are described in the experimental design section. The third step is discussed below.

For a classified image (or a map), a confusion matrix (also called an error matrix or a contingency table) can be made by comparing the classification results with reference data. In this matrix, the reference data are represented by the columns of the matrix while the classified data are represented by the rows, or *vice versa*. The major diagonal of the confusion matrix indicates the agreement between these two data sets. The confusion matrix allows various accuracy indices to be derived (e.g., Fung and LeDrew, 1988; Rosenfield and Fitzpatrick-Lins, 1986).

In this paper, only the confusion matrix, the producer's and user's single-class accuracy (Story and Congalton, 1986), and the overall accuracy were used.

## 3. EIGEN-BASED GREY-LEVEL VECTOR REDUCTION

As explained in the above section, in order to make better use of the frequency-based classification technique, the number of grey-level vectors in multispectral space has to be reduced. The simplest way of doing this is by compressing the number of grey levels in each band of the image. In this section, it is demonstrated that grey-level vector reduction in multispectral space is not appropriate. A more efficient method that is done in eigenvector space will be described.

### 3.1. GREY-LEVEL VECTOR REDUCTION IN MULTISPECTRAL SPACE

The easiest way to reduce the number of grey-level vectors is to compress the number of grey levels in *each individual* spectral band. More sophisticated grey-level reduction algorithms exist for each individual band. For instance, Sezan (1990) proposed an algorithm that locates peaks and valleys from a histogram of an image. However, since the peaks and valleys are not located in equal distance, the precise distance metric in multispectral space is lost and this will make the distance measures useless in the classification stage. Algorithms such as Sezan's may only prove useful for image display purposes where qualitative grey-level differences are required.

### 3.2. GREY-LEVEL VECTOR REDUCTION IN EIGEN SPACE

It is well known that some bands of multispectral image are highly correlated. Principal component (PC) transformation can reduce the data redundancy effectively through transforming the data from multispectral space to the eigenvector space of the data (e.g., Richards, 1986). Since the data variability is to be preserved for discrimination purposes, only the first few principal components need to be kept for multispectral data. This results in a reduction of data dimension and therefore reduces the amount of data to be handled.

However, Gong and Howarth (1992) demonstrated that simply reducing the dimensionality of the data is not sufficient if frequency tables are to be used in the classification. Therefore a new grey-level vector reduction algorithm has been developed. It has the desirable performance of balancing the information loss in the eigen space and preserving the eigen structure of the original data while conducting grey-level vector reduction. As an example for illustration purposes, Figure 1 shows the generalized eigen structure of the SPOT HRV data that were used in Gong and Howarth (1992). In this figure, only the first two eigen vectors and the plane they constructed are shown. The variance in the third PC is too small to be considered. Our focus is on partitioning the preserved eigen plane. Figure 2 shows a partition of the preserved eigen plane with equal quantization of eight grey levels. It is obvious that along the second eigen axis there are too many partitions which make grey-level cells on the preserved eigen plane become rectangular. The partitioning method proposed in Gong and Howarth (1992) is shown in Figure 3. Because there is more variation along the first eigen axis than there is along the second eigen axis, there are more grey-level partitions on the first eigen axis than on the second axis.

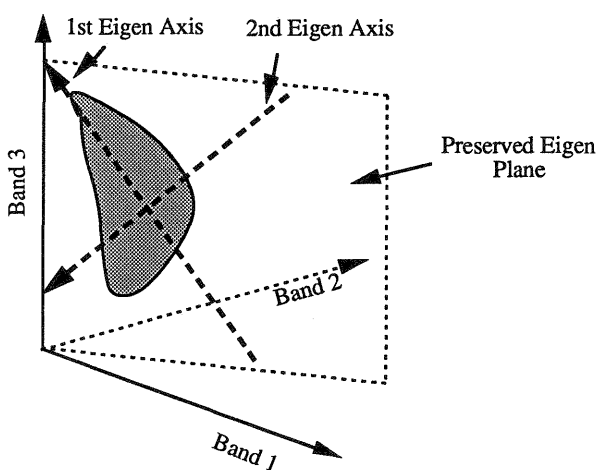


FIG. 1. Eigen structure of the SPOT HRV data used in this study.

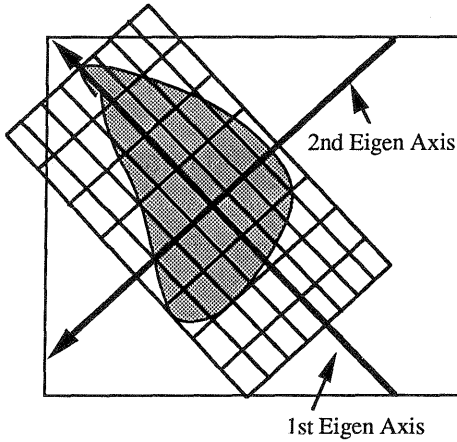


FIG. 2. Partition of the eigen space into equal grey levels along each eigen vector.

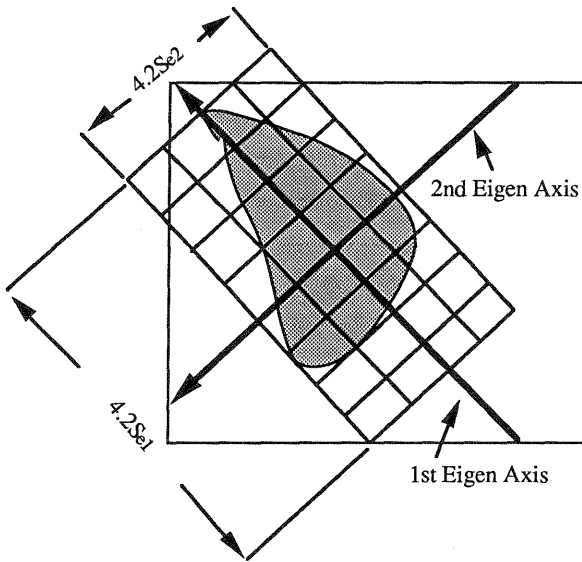


FIG. 3. Partition of the eigen space using the method proposed in this study.

The grey-level vector-reduction scheme can be formalized and generalized. Given the covariance matrix and the mean grey-level vector,  $M = (m_1, m_2, \dots, m_k)^T$ , calculated from  $k$  multispectral bands of the image, the multispectral coordinates from multispectral space  $S^k$  can be rotated into eigen coordinates in eigen space  $E^k$  (Richards, 1986). Let  $V_1, V_2, \dots, V_k$  represent the eigenvectors. A grey-level vector,  $G = (g_1, g_2, \dots, g_k)^T$ , in multispectral space can be transformed into a grey-level vector,  $G_e = (v_1, v_2, \dots, v_k)^T$ , in eigen space. This can be obtained from:

$$\begin{pmatrix} v_1 \\ v_2 \\ \vdots \\ v_k \end{pmatrix} = (V_1, V_2, \dots, V_k)^T \begin{pmatrix} g_1 \\ g_2 \\ \vdots \\ g_k \end{pmatrix}$$

Let  $s_{e1}^2, s_{e2}^2, \dots, s_{ek}^2$  represent the eigenvalues corresponding to each eigenvector. These eigenvalues are the variances along each eigen vector direction in eigen space. In order to keep the same signal to noise level between eigen axes (e.g., to make square cells on the eigen plane in Figure 3), our partition of eigen space is so designed that the number of grey levels along each eigenvector is proportional to the square root of its corresponding eigenvalue. That is:

$$\frac{N_{e1}}{S_{e1}} = \frac{N_{e2}}{S_{e2}} = \dots = \frac{N_{ek}}{S_{ek}}$$

where  $N_{e1}, N_{e2}, \dots, N_{ek}$  are the numbers of grey levels used for each corresponding eigenvector. As can be seen from the above equations, we have only  $k-1$  equations but  $k$  unknown variables  $N_{e1}, N_{e2}, \dots, N_{ek}$ . To determine all the  $k$  unknowns, one condition is added:

$$N_{e1} \cdot N_{e2} \cdot \dots \cdot N_{ek} = N_E$$

where  $N_E$  is the total number of grey-level vectors to be expected for the partition of the eigen space.

To implement the eigen space partition, the origin of the eigen space (the same as the origin in multispectral space) needs to be shifted to the new origin  $E_o = (e_1, e_2, \dots, e_k)^T$  which is the mean grey-level vector  $M$  in multispectral space.  $E_o$  is obtained through the following:

$$\begin{pmatrix} e_1 \\ e_2 \\ \vdots \\ e_k \end{pmatrix} = (V_1, V_2, \dots, V_k)^T \begin{pmatrix} m_1 \\ m_2 \\ \vdots \\ m_k \end{pmatrix}$$

Where the partition starts and how far apart each grey-level interval is along an eigen axis can now be determined.  $2.1 S_{ei}$  at each side of the origin along eigen axis  $i$  were selected as the starting and ending points for the grey-level partition. This was determined from the normal distribution curve by assuming data were normally distributed along each eigen axis. Based on this assumption, the use of 2.1 guarantees 97 percent of the grey-level vectors in multispectral space fall into the range  $[-2.1 S_{ei}, +2.1 S_{ei}]$  on eigen axis  $i$ . The remainder (less than 3 percent) will fall outside the range. Depending on the actual data distribution, the number "2.1" can be slightly adjusted to keep a majority of grey-level vectors falling into the specified range. The grey levels along each eigen axis are numbered in an ascending order from 0 with an increment of 1 to  $N_{ei}-1$ . Figure 4 illustrates the division of the  $i$ th eigen axis into  $N_{ei}$  grey levels.

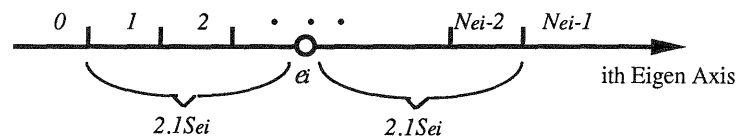


FIG. 4. Division of an eigen axis into a specific number of grey levels.

By dividing each eigen axis into the number of grey levels obtained above, the original multispectral space will be partitioned into  $N_E$  pieces or grey-level vectors in eigen space. The purpose, which is to reduce the large number of grey-level vectors in multispectral space, will therefore be achieved. From the transformed grey-level vector of a pixel,  $G_e = (v_1, v_2, \dots, v_k)^T$ , the reduced grey-level vector,  $G_r = (r_1, r_2, \dots, r_k)^T$ , can be obtained according to the division along each eigen axis, as described above. For example,  $r_1$  is reduced from  $v_1$  according to the following rule:

$$a = (v_1 - e_1 + 2.1S_{e1})(N_{e1} - 2) / 4.2S_{e1} + 1$$

$$r_1 = \begin{cases} 0 & \text{if } a \leq 1 \\ N_{e1} - 1 & \text{if } a > N_{e1} - 2 \\ a & \text{else} \end{cases}$$

In order to allow the frequency-based classification algorithms easy access to the data after grey-level vector reduction, it was decided to use only one image to store the data. A labeling system was developed to assign a number to each grey-level vector created in eigen space. A number  $n_e$  for a particular grey-level vector,  $G_r = (r_1, r_2, \dots, r_k)^T$ , is calculated according to the following equation:

$$n_e = r_k \cdot N_{e1} \cdot N_{e2} \cdot \dots \cdot N_{e(k-1)} + r_{k-1} \cdot N_{e1} \cdot N_{e2} \cdot \dots \cdot N_{e(k-2)} + \dots + r_1$$

After this labeling, all the partitioned grey-level vectors in eigen space will range from 0 to  $N_E - 1$ .

In summary, it takes four steps to obtain reduced grey-level vectors using the new algorithm. In the first step, the algorithm generates the covariance matrix and mean grey-level vector from the original multispectral image by using either samples or the entire image. In the second step, the eigen values and their corresponding eigen vectors are derived from the covariance matrix. In the third step, the eigen space is partitioned into an expected number ( $N_E$ ) of pieces. Finally, the grey-level values of every pixel in the multispectral image are transformed into the eigen space and each pixel is assigned a new grey-level vector number ( $n_e$ ). The assignment is done according to the section (new grey-level vector) in the partition of the eigen space into which the transformed coordinates of each pixel fall.

#### 4. EXPERIMENTAL DESIGN

The proposed algorithms were originally implemented with the FORTRAN 77 programming language on a VAX 11/785 computer under the VMS operating system. It has been transported and rewritten as an additional module of PCI's EASI/PACE image analysis software. In this section, the study site and the land-use classification scheme are introduced. The training strategy and the test sample selection will then be described.

##### 4.1. STUDY SITE AND LANDSAT TM DATA

The study site is Kitchener-Waterloo, Ontario, Canada and its surrounding area. This site has been used for a variety of remote sensing studies of land-cover/land-use changes (e.g., Gong, et al., 1992; Fung and LeDrew, 1988).

The Landsat TM image (Path-Row No. 18-30) was acquired on 3 August 1985. For this research, a cloud-free subscene of 256 by 512 pixels was selected. Since the selected test site is small

and relatively flat, both topographic and atmospheric conditions were assumed to be homogeneous throughout the image. Based on these assumptions, there is little or no topographic effect on the data and any atmospheric effects on the data are homogeneous in the study area. They can be considered as a contribution from atmospheric haze. To remove homogeneous haze effects from each band of the image requires only the subtraction of a constant from each pixel value. However, this would not change the radiometric structure of the data. In addition, the subsequent classifications used in this study are statistically invariant to linear transformations. Thus, no radiometric correction was made to the image.

##### 4.2. LAND-USE CLASSIFICATION SCHEME

The land-use classification scheme is listed in Table 1.

TABLE 1. LAND-USE CLASSIFICATION SCHEME

Land Use Class	Code
Old Urban Residential	RES1
New Urban Residential	RES2
Industrial/Commercial	IND/COM
Institutional	INST
Cleared Land	CLEAR
Crop and Pasture	CROP
Idle land	IDLE
Water	WATER
Golf Course	GOLF
Parks	PARK

These land-use classes are typically found among North-American cities. A structural description and spectral characteristics of these land-use types are found in Gong and Howarth (1992).

##### 4.3. SUPERVISED TRAINING TEST-SAMPLE SELECTION

The training procedure used in this research is straightforward. In order to achieve maximum flexibility, it was decided to use a block-training strategy. The advantage of this type of training is its ease in specifying training areas. By so doing, the image analyst also implicitly identifies the spatial structure for a particular class. The shape and the size of the training block contain important clues for selecting the appropriate pixel window size to be used in generating frequency tables. Test sample selection procedure was the same as in the training process, but test samples were not overlapping with the training sites. Therefore, bias on final estimates of classification accuracies can be avoided.

##### 4.4. GENERATION OF GREY-LEVEL VECTOR-REDUCED IMAGES

With the grey-level vector-reduction algorithm, the original six bands (TM 1-5 and TM 7) of Landsat TM image can be reduced to one image. Two factors affect the resultant grey-level vector-reduced images. They are the method used to calculate the covariance matrix for constructing the eigen space, and the number of grey-level vectors specified for the output image. More detail on these factors can be found in Gong and Howarth (1992).

The number of grey-level vectors specified for the output image determines how much detail from the original image is to be preserved in the output image. For this experiment, the grey-level vector number of 50 was tested. The algorithm was designed in such a manner that it is independent of changes in the number of grey-level vectors specified.

#### 4.5. LAND-USE CLASSIFICATION

For the grey-level vector-reduced image, a pixel window of 9 X 9 was used in the land-use classification. For comparison purposes, a maximum-likelihood classifier (MLC) was applied to the six-band Landsat TM image while training and test samples were the same as in the frequency-based classification.

### 5. RESULTS AND DISCUSSION

#### 5.1. LAND-USE CLASSIFICATION RESULTS OBTAINED USING A MAXIMUM-LIKELIHOOD CLASSIFIER

Table 2 shows the confusion matrix, the producer's and the user's accuracies, and the overall classification accuracies obtained with the MLC. The codes in the row and column entries in Table 2 represent the land-use classes as listed in Table 1.

TABLE 2. CONFUSION MATRIX AND CLASSIFICATION ACCURACIES OBTAINED USING THE MLC

	RES1	RES2	INCO	INST	CL	CROP	IDLE	WATR	GOLF	PARK	USER
RES1	446	97	1	5					3	16	78.52
RES2	57	444	19	34	1				2	1	79.57
IND/COM	2	1	404	50	1						88.21
INST	7	28	33	191	13					1	69.96
CLEAR		1	2	11	260						94.89
CROP						219			15		93.59
IDLE		1		5	1		145				95.39
WATER								93			100
GOLF	2	1							355	7	97.26
PARK	54	28		1		4	1		24	88	44.00
PRODUCER	78.50	73.90	86.70	64.09	94.20	97.80	99.30	100	89.00	77.90	
ΣColumn	568	601	459	297	276	223	146	93	399	113	
OVERALL	83.31										

TABLE 3. CONFUSION MATRIX FOR THE LAND-USE MAP PRODUCED FROM THE GREY-LEVEL VECTOR REDUCED IMAGE WITH A PIXEL WINDOW SIZE OF 9

	RES1	RES2	INCO	INST	CL	CROP	IDLE	WATR	GOLF	PARK	USER
RES1	539									5	99.08
RES2	6	601	10				6				96.47
IND/COM			428	2							99.53
INST			28	287	13						87.50
CLEAR					263						100
CROP						224					100
IDLE				9			140				93.96
WATER								96			100
GOLF									399		100
PARK	23									108	82.44
PRODUCER	94.89	100	91.85	96.31	95.29	100	95.89	100	100	95.58	
ΣColumn	568	601	466	298	276	224	146	96	399	113	
OVERALL	96.80										

#### 5.2. LAND-USE CLASSIFICATION RESULTS OBTAINED FROM GREY-LEVEL VECTOR-REDUCED IMAGES

Table 3 shows the confusion matrix, the producer's and the user's accuracies, and the overall classification accuracies generated from grey-level vector-reduced image using the Gong-Howarth contextual classification method. It can be seen from Table 3 that for Gong-Howarth method accuracies from 8 land-use classes have been improved considerably as compared with the results obtained with the MLC. The only class whose accuracy has been slightly reduced is class IDLE. The reason for this has been explained in Gong and Howarth (1992) that the spectral characteristics of land-use classes such as IDLE are relatively pure and such classes can be more appropriately classified using single-pixel classification algorithms such as the MLC. The overall classification accuracy has been dramatically improved from 83.31% obtained with the MLC to 96.80% due to the use of the Gong-Howarth classification method.

#### 5.3. THE POTENTIAL OF THE GREY-LEVEL VECTOR-REDUCTION ALGORITHM IN CLUSTERING

Based on the grey-level vector-reduction algorithm, a clustering procedure can be developed. It will be similar to a conventional c-means clustering algorithm, but instead of clustering in

multispectral space, the clustering can be done in eigen space with reduced grey-level vectors.

In the final step of the algorithm for grey-level vector reduction, after all pixels have been assigned a reduced grey-level vector number, an average of  $G_e$ 's for all pixels that fall into the same reduced grey-level vector is calculated. Let  $G_a(i) = (a_1, a_2, \dots, a_k)^T$ , denotes the average for those pixels falling into the reduced grey-level vector  $i$ ,  $i = 0, 1, \dots, N_E - 1$ . These  $N_E$  average grey-level vectors can then be clustered. Because  $N_E$  is relatively small, the clustering process can be extremely fast. Some properties of this clustering method is under investigation.

## 6. SUMMARY AND CONCLUSIONS

The Gong-Howarth contextual classification method has been tested to classify a urban environment using the Landsat TM data obtained over. It involves two steps: grey-level vector reduction and frequency-based classification. The algorithms can be easily modified to conduct fast clustering.

Test results of this study indicate that the Gong-Howarth contextual classification method can considerably improve urban land-use classification accuracies with Landsat TM data.

Further research will be directed to reduce the pixel window effect as discussed in Gong and Howarth (1992).

## 7. ACKNOWLEDGEMENTS

This research was funded by an NSERC research Grant from the Natural Science and Engineering Research Council of Canada and a starter grant from The University of Calgary awarded to P. Gong. PCI Inc. provided the author with their EASI/PACE image analysis software.

## 8. REFERENCES

- Fung, T., and E. F. LeDrew, 1988. The determination of optimal threshold levels for change detection using various accuracy indices. *Photogrammetric Engineering and Remote Sensing*, 54(10):1449-1454.
- Gong, P., and P. J. Howarth, 1992. Frequency-based contextual classification and grey-level vector reduction for land-use identification. *Photogrammetric Engineering and Remote Sensing*, 58(4):423-437.
- Gong, P., E.F. LeDrew, and J.R. Miller, 1992. Registration-noise reduction in difference images for change detection, *International Journal of Remote Sensing*, 13(5):773-779.
- Gong, P., D. Marceau and P. J. Howarth, 1992, A comparison of spatial feature extraction algorithms for land-use classification with SPOT HRV data. *Remote Sensing of Environment*. 40:137-151.
- Gonzalez, R. C., and P. Wintz, 1987. *Digital Image Processing*, Second Edition. Addison-Wesley Publishing Company, Reading, Mass.
- Richards, J. A., 1986. *Remote Sensing Digital Image Analysis: An Introduction*. Springer-Verlag, Berlin.
- Rosenfield, G. H., and K. Fitzpatrick-Lins, 1986. A coefficient of agreement as a measure of thematic classification accuracy. *Photogrammetric Engineering and Remote Sensing*, 52(2):397-399.
- Sezan, M. I., 1990. A peak detection algorithm and its application to histogram-based image data reduction. *Computer Vision, Graphics, and Image Processing*, 49:36-51.
- Story, M., and R. G. Congalton, 1986. Accuracy assessment: a user's perspective. *Photogrammetric Engineering and Remote Sensing*, 52(3):223-227.